

# UC Irvine

## UC Irvine Previously Published Works

### Title

First results from solid state neutral particle analyzer on experimental advanced superconducting tokamak.

### Permalink

<https://escholarship.org/uc/item/5tn7624p>

### Journal

The Review of scientific instruments, 87(11)

### ISSN

0034-6748

### Authors

Zhang, JZ  
Zhu, YB  
Zhao, JL  
[et al.](#)

### Publication Date

2016-11-01

### DOI

10.1063/1.4962063

### Copyright Information

This work is made available under the terms of a Creative Commons Attribution License, available at <https://creativecommons.org/licenses/by/4.0/>

Peer reviewed

# First results from solid state neutral particle analyzer on experimental advanced superconducting tokamak

J. Z. Zhang,<sup>1</sup> Y. B. Zhu,<sup>2,a)</sup> J. L. Zhao,<sup>1</sup> B. N. Wan,<sup>1</sup> J. G. Li,<sup>1</sup> and W. W. Heidbrink<sup>2</sup>

<sup>1</sup>*Institute of Plasma Physics, Chinese Academy of Sciences, Hefei 230031, China*

<sup>2</sup>*Department of Physics and Astronomy, University of California, Irvine, California 92697, USA*

(Presented 7 June 2016; received 3 June 2016; accepted 19 August 2016; published online 2 September 2016)

Full function integrated, compact solid state neutral particle analyzers (ssNPA) based on absolute extreme ultraviolet silicon photodiode have been successfully implemented on the experimental advanced superconducting tokamak to measure energetic particle. The ssNPA system has been operated in advanced current mode with fast temporal and spatial resolution capabilities, with both active and passive charge exchange measurements. It is found that the ssNPA flux signals are increased substantially with neutral beam injection (NBI). The horizontal active array responds to modulated NBI beam promptly, while weaker change is presented on passive array. Compared to near-perpendicular beam, near-tangential beam brings more passive ssNPA flux and a broader profile, while no clear difference is observed on active ssNPA flux and its profile. Significantly enhanced intensities on some ssNPA channels have been observed during ion cyclotron resonant heating. *Published by AIP Publishing.* [<http://dx.doi.org/10.1063/1.4962063>]

## I. INTRODUCTION

Energetic particles (EPs) related to fusion reactions, neutral beam injection (NBI) and/or ion cyclotron resonant heating (ICRH) auxiliary heating, and magnetohydrodynamics (MHD) instabilities play a major role in tokamak hot plasma.<sup>1</sup> By measuring charge-exchange (CX) fast neutrals escaped from plasmas, neutral particle analyzer (NPA) is an essential tool for diagnosing and studying the important EP behaviors.<sup>2,3</sup>

Conventional NPAs are comparatively large, complicated, and expensive.<sup>3,4</sup> It is impractical to build and maintain a multi-channel diagnostic system on the tokamak in very limited available space. Recent development on compact solid state neutral particle analyzers (ssNPA) based on absolute extreme ultraviolet (AXUV) silicon photodiode<sup>5</sup> are very attractive because they are small in size, simple to operate, and low cost.<sup>6–12</sup> The full function integrated ssNPA system based on specially fabricated AXUV detectors with fast response and ultra-high vacuum (UHV) compatibility has been designed and installed for the first time on experimental advanced superconducting tokamak (EAST) in 2014,<sup>6</sup> based on the experience obtained from previous individual development such as advanced current mode operation on DIII-D,<sup>7</sup> coarse pulse height spectrum measurements on national spherical torus experiment (NSTX),<sup>8,9</sup> and other devices.<sup>10–12</sup>

EAST, equipped now with two 50–80 keV 4 MW NBI and two 24–70 MHz 6 MW ICRH system, provides an excellent platform for EP study after recent significant upgrades.<sup>13</sup> In this article, implementation and typical operational experience of the ssNPA system on EAST are described in detail in Sec. II.

Some experimental results obtained from this diagnostic are reported in Sec. III. Finally, Sec. IV is a brief summary and future plan.

## II. DIAGNOSTIC SETUP AND OPERATION

The two vertical ssNPA ports ( $B^{\text{up}}$  and  $N^{\text{up}}$ ) and two 16-channel horizontal ssNPA sightlines from midplane port P together with four NBI beam-lines (#1 from port A, #2 from port F) and two ICRH ports (B and I) are illustrated on Figure 1(a).

### A. Horizontal ssNPA arrays

The assembly of the two horizontal ssNPA arrays is shown in Figure 1(b) as computer-aided drafting (CAD) drawing. Heavy duty linear motion UHV compatible feedthrough is employed to hold two detector chambers (cameras) and could be manually pulled back up to 30 cm to protect the detectors from harsh environment near the first wall during vacuum baking and lithium-powder dropping. The rotary manual actuator provides position indication and is locked at marked position during normal ssNPA operation.

This retractable system design has proven effective to keep detectors from contaminants and below a 100 °C temperature limit, without the complications of a shutter and active cooling. Eight thermocouples are mounted on the detector chamber for temperature measurement. The maximum temperature measured near the detector is 89 °C while the EAST baking gas is set at 250 °C. No clear contamination has been found on the detector arrays even after kilogram scale of lithium has been consumed for wall-conditioning in 2015 experimental campaign. The insides of detector chambers are still clean while the outside is covered with massive amounts of grayish lithium.

Two AXUV16ELG arrays with direct deposition of 100 nm tungsten (W) foil on sixteen 2 mm × 5 mm

Note: Contributed paper, published as part of the Proceedings of the 21st Topical Conference on High-Temperature Plasma Diagnostics, Madison, Wisconsin, USA, June 2016.

<sup>a)</sup>Author to whom correspondence should be addressed. Electronic mail: y.zhu@uci.edu.

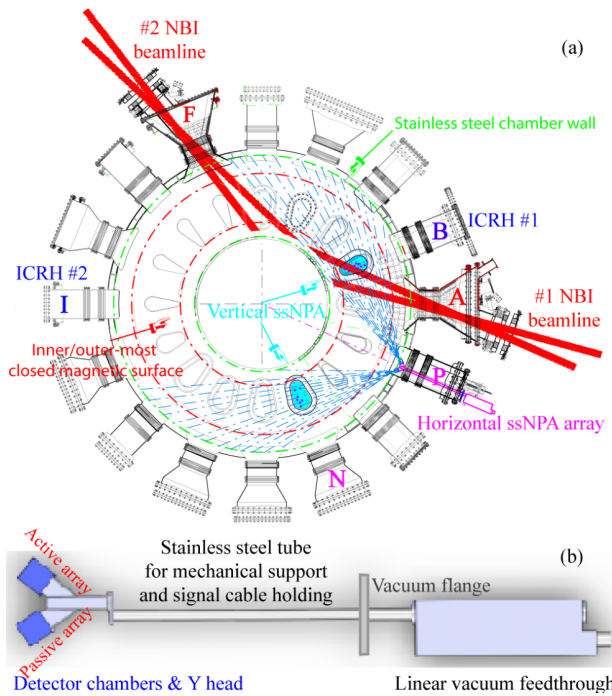


FIG. 1. (a) Top view of the EAST with ssNPA ports and sightlines, NBI footprints, and ICRH port locations. (b) Schematic CAD drawing for horizontal ssNPA arrays.

photodiode elements are installed inside each chamber on the Y head. Each element is located at about 15 cm below EAST equatorial plane and views the plasma through a  $9 \text{ mm} \times 1 \text{ mm}$  aperture. The counter-clockwise ssNPA view-chords intersect both near-tangential and near-perpendicular footprints of NBI #1, providing active CX measurements. The other ssNPA array with toroidally mirrored view-chords faces clockwise, missing all four NBI footprints, to provide passive CX measurements.

## B. Vertical individual channels

As shown in Figure 2, seven individual W-foil deposited AXUV20HS1 detectors, each with  $19.7 \text{ mm}^2$  active area, are mounted on  $N^{\text{up}}$  vertical port. To provide passive CX measurements, these channels miss all NBI footprints. Five of nine vertical channels on  $B^{\text{up}}$  port intersect NBI #1 footprints to provide active CX measurements; the other four channels operate in passive mode. (See Figure 3 in Ref. 6.) Each channel is equipped with a 0.5 m long  $\varnothing 8 \text{ mm}$  stainless steel guiding tube that includes collimation apertures. No extra protection is necessary because all detectors are suspended near the port's top flanges, about 4 m from EAST midplane.

## C. Electronics, data acquisition (DAQ) and operation

The detectors' output is sent to 32-pin UHV compatible electrical feedthroughs that feed current to voltage amplifiers on the atmosphere side through 32-core twisted-pair shielded cables. In order to improve the signal to noise ratio and signal bandwidth, the distance between the detector and transimpedance preamplifier is minimized (1.5 m long for horizontal arrays and 0.5 m for vertical channels). The signals after amplifiers are transmitted by twisted-pair shielded cables to the EAST general data acquisition (DAQ) system.

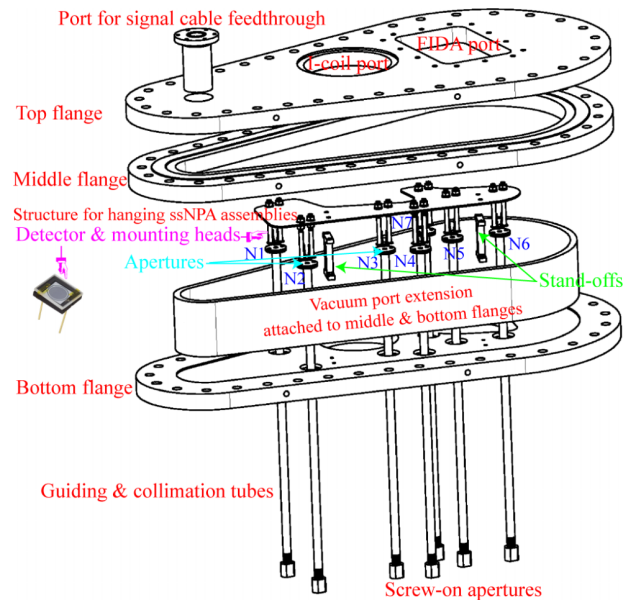


FIG. 2. CAD drawing for ssNPA assembly on  $N^{\text{up}}$  vertical port.

Two homemade 16-channel front-end transimpedance amplifiers and one 32-channel second stage voltage amplifier<sup>14</sup> are used for horizontal arrays, with considerations on budget and space saving. The total gain is about  $10^5 \text{ V/A}$ . For flexibility, commercial individual transimpedance amplifiers are used for all 16 vertical channels. The normal setup is  $10^6 \text{ V/A}$ , while each amplifier provides selectable gain from  $10^5$  to  $10^8 \text{ V/A}$ .

Small Computer System Interface SCSI-3 to BNC adapters are used to match to the EAST DAQ system. Presently, the ssNPA DAQ supports 48 14-bit channels with 200 kHz sampling rate and  $[-10, +10] \text{ V}$  input. All data are stored in EAST MDSplus server.

Up to now, all channels are operated in advanced current mode for fast time resolution measurement. The vertical amplifier's gain is one order higher than the horizontal channel's, because it has smaller neutral particle influx from (1) longer distance between the vertical detectors and plasma, (2) the view cone's effective volume limited by the 0.5 m long guiding tube.

## III. PRELIMINARY EXPERIMENTAL RESULTS

The ssNPA system has been successfully operated and continuously improved since it was first commissioned in the EAST 2014 experiment campaign. The well-conditioned ssNPA system is ready for dedicated EP physics experiments. Data shown below are from detectors with 100 nm W filter, which has a low energy detection threshold of 22 keV for deuterium and 26 keV for hydrogen.

Figure 3 shows a typical temporal evolution of the ssNPA flux's profile from the horizontal active array while tangential and perpendicular branches from NBI #1 are modulated at 500 ms 50% duty cycle. The ssNPA signal increases substantially when the beam turns on; the flux profile strongly correlates with the injected NBI. The profile shows a peak near the plasma center (around channel 9) and gradually broadens in time during the injection of the 60 keV neutral deuterium beam. Gradual broadening is also evident during each individual beam pulse.

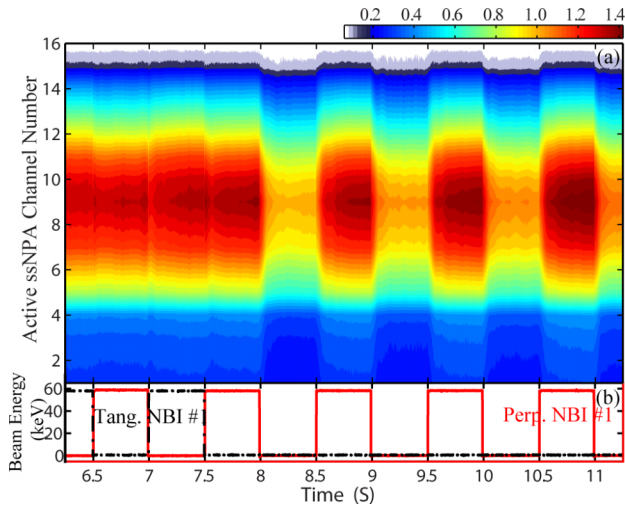


FIG. 3. Temporal evolution of (a) active ssNPA flux profile and (b) energy of tangential and perpendicular NBI #1, for #62810.

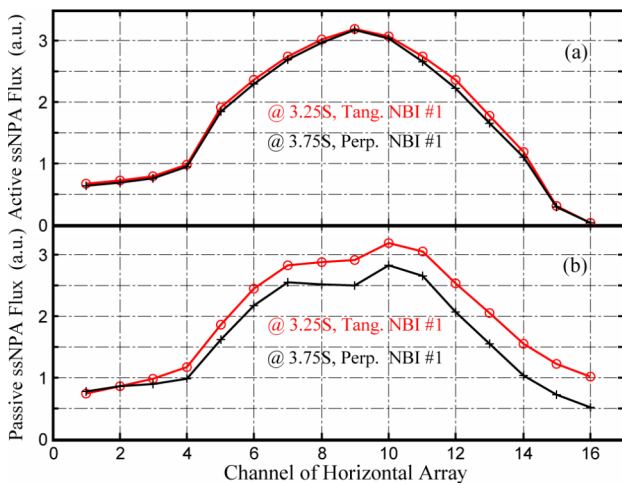


FIG. 4. Flux profiles from the (a) active and (b) passive ssNPA arrays with only tangential and perpendicular NBI #1 turned on, for #59474.

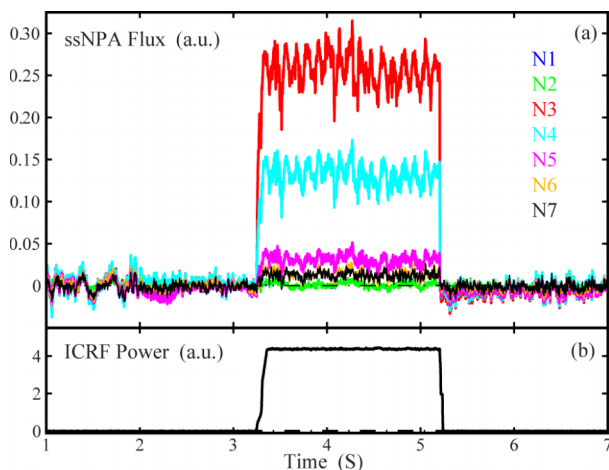


FIG. 5. Temporal evolution of (a) vertical ssNPA flux at port  $N^{\text{up}}$  and (b) injected ICRF power, for #65100.

Active and passive ssNPA profiles are compared in Figure 4. Tangential and perpendicular NBI are alternately turned on and off for active CX measurements. The active ssNPA flux is virtually unchanged for each channel, and its profile is insensitive to injected beam source. In contrast, the passive ssNPA flux is larger with the tangential beam than with the perpendicular beam, and its profile is broader during tangential beam injection.

Figure 5 illustrates time traces of the passive ssNPA flux on vertical  $N^{\text{up}}$  port together with ICRH power. Compared to other channels, the significantly enhanced intensities on channels N3 and N4 show evidence for a resonant perpendicular heating effect.

#### IV. SUMMARY AND FUTURE PLAN

The new integrated ssNPA system with both active and passive measurement capabilities has been implemented and successfully commissioned on EAST. The design of individual vertical channels together with mirrored horizontal arrays on retractable feedthrough has proven effective. The reasonable strong correlation between ssNPA signals and injected power from NBI as well as ICRH indicates that the ssNPAs are ready for dedicated EP experiments.

In the near future, a dedicated DAQ system will be developed, for continuous data acquisition with sampling rate up to 500 kHz. Meanwhile, a few vertical individual channels will be operated in pulse-counting mode to measure the wider EP spectroscopy for ICRH plasmas.

#### ACKNOWLEDGMENTS

Work supported jointly by National Magnetic Confinement Fusion Energy Research Program of China under Grant Nos. 2011GB101004, 2015GB110005, and 2014GB109004, the National Natural Science Foundation of China under Grant Nos. 11628509 and 11575249, and the US Department of Energy under Grant No. SC-G903402. Contributions and encouragement from G. Q. Zhong, Y. M. Duan, F. Wang, D. Liu, C. D. Hu, B. J. Xiao, and L. Q. Hu are highly appreciated.

<sup>1</sup>A. Fasoli *et al.*, *Nucl. Fusion* **47**, S264 (2007).

<sup>2</sup>J. Wesson, *Tokamaks*, 4th ed. (Oxford University Press, 2011).

<sup>3</sup>S. S. Medley, A. J. H. Donné, R. Kaita, A. I. Kislyakov, M. P. Petrov, and A. L. Roquemore, *Rev. Sci. Instrum.* **79**, 011101 (2008).

<sup>4</sup>A. I. Kislyakov and M. P. Petrov, *Plasma Phys. Rep.* **35**, 535 (2009).

<sup>5</sup>See <http://optodiode.com/products.html> for more information about AXUV silicon photodiode.

<sup>6</sup>Y. B. Zhu, J. Z. Zhang, M. Z. Qi, S. B. Xia, D. Liu, W. W. Heidbrink, B. N. Wan, and J. G. Li, *Rev. Sci. Instrum.* **85**, 11E107 (2014).

<sup>7</sup>Y. B. Zhu, A. Bortolon, W. W. Heidbrink, S. L. Celle, and A. L. Roquemore, *Rev. Sci. Instrum.* **83**, 10D304 (2012).

<sup>8</sup>D. Liu, W. W. Heidbrink, D. S. Darrow, A. L. Roquemore, S. S. Medley, and K. Shinohara, *Rev. Sci. Instrum.* **77**, 10F113 (2006).

<sup>9</sup>K. Shinohara, D. S. Darrow, A. L. Roquemore, S. S. Medley, and F. E. Cecil, *Rev. Sci. Instrum.* **75**, 3640 (2004).

<sup>10</sup>V. Tang *et al.*, *Rev. Sci. Instrum.* **77**, 083501 (2006).

<sup>11</sup>M. Osakabe *et al.*, *Rev. Sci. Instrum.* **72**, 788 (2001).

<sup>12</sup>T. Yamamoto *et al.*, *Rev. Sci. Instrum.* **72**, 615 (2001).

<sup>13</sup>B. N. Wan, J. G. Li, H. Y. Guo, Y. F. Liang, G. S. Xu, L. Wang, X. Z. Gong, A. Garofalo, and EAST Team and Collaborators, *Nucl. Fusion* **55**, 104015 (2015).

<sup>14</sup>D. Liu, W. W. Heidbrink, K. Tritz, Y. B. Zhu, A. L. Roquemore, and S. S. Medley, *Rev. Sci. Instrum.* **85**, 11E105 (2014).